

Received June 11, 2021, accepted July 2, 2021, date of publication July 8, 2021, date of current version July 16, 2021.

Digital Object Identifier 10.1109/ACCESS.2021.3095720

Physical Modeling of the Ancient Greek Wind Musical Instrument Aulos: A Double-Reed Exciter Linked to an Acoustic Resonator

SPYROS POLYCHRONOPOULOS¹, DIMITRA MARINI¹, KONSTANTINOS BAKOGIANNIS¹,
GEORGIOS TH. KOUROUPETROGLOU¹, (Member, IEEE), STELIOS PSAROUDAKĒS²,
AND ANASTASIA GEORGAKI²

¹Department of Informatics and Telecommunications, National and Kapodistrian University of Athens, 15784 Athens, Greece

²Department of Music Studies, National and Kapodistrian University of Athens, 15784 Athens, Greece

Corresponding author: Georgios Th. Kouroupetroulou (koupe@di.uoa.gr)

This work was supported by the European Regional Development Fund of the European Union and Greek National funds through the Operational Program Competitiveness, Entrepreneurship, and Innovation (under the call Research-Creat-Innovate Project MNESIAS: "Augmentation and enrichment of cultural exhibits via digital interactive sound reconstitution of ancient Greek musical instruments") under Grant T1EDK-02823 / MIS 5031683.

ABSTRACT We present a simulation method for the auralization of the ancient Greek double-reed wind instrument Aulos. The implementation is based on Digital Signal Processing and physical modeling techniques for the instrument's two parts: the excitation mechanism and the acoustic resonator with toneholes. Single-reeded instruments are in-depth studied firstly because their excitation mechanism is the one used in a great amount of modern wind-reed instruments and secondly because the physics governing the phenomena is less complicated than the double-reeded instruments. We here provide a detailed model of a system comprised of a double-reed linked to an acoustic resonator with toneholes to sonify Aulos. We validate our results by comparing our method's synthesized signal with recordings from a replica of Aulos of Poseidonia built in our lab. The comparison showed that the fundamental frequencies and the first three odd harmonics of the signals differ 6, 5, 3, and 2 cents on average, respectively, which is below the Just Noticeable Difference threshold.

INDEX TERMS Aulos, digital signal processing, digital waveguides, double-reed, musical acoustics.

I. INTRODUCTION

The realistic sonification of physical musical instruments by digital means constitutes a pole of attraction in several multidisciplinary scientific fields, such as physics, informatics, musicology [1]–[7]. Theoretical acoustics has significantly contributed to a better understanding of the physical phenomena governing the generated sound. On the other hand, computer scientists have developed new cost-effective algorithms running under modern and user-friendly interfaces, which can simulate the phenomena and achieve real-time sonification. These applications are not only valuable for musicians but to the instrument industry as well. Influential pieces of software that, via digital simulation, sonify a virtually customized musical instrument are now commercially available, allowing

accurate pre-production testing without physically building the instrument.

State-of-the-art physical modeling (PM) techniques [8]–[10] have been put into practice by commercial companies (Native Instruments,¹ Modartt,² Applied Acoustic Systems,³ etc.) to realistically sonify various popular instruments. Distinct simulation techniques of single-reed wind instruments have been proposed [11]–[15], leading to the development of commercial pieces of software (e.g., Swam Clarinets⁴). The nonlinear phenomena introduced by the oscillating reed [11], [14], [16], [17] and the linear effect of the oscillating air volume inside the resonator [12], [14], [15],

¹<https://www.native-instruments.com/>

²<https://www.modartt.com/>

³<https://www.applied-acoustics.com/>

⁴<https://audiomodeling.com/swam-engine/solo-woodwinds/swam-clarinets/>

The associate editor coordinating the review of this manuscript and approving it for publication was Derek Abbott¹.

which defines the resonance and therefore the pitch and timbre of the produced sound, are the fundamental elements governing the physical phenomena of the reed wind instrument. We assumed that these elements are the fundamental aspects of significance in our model and validated the claim with the results.

The resonator (a cavity where air particles that transmit the sound waves are enclosed) of the majority of wind instruments is either a cylindrical pipe or a conical horn. We note here that Aulos (cylindrical resonator) and oboe (conical resonator) have rather different harmonics even if both instruments had the same resonator's length. The air column oscillates with respect to the tube's resonant frequency, which is determined by the instrument's geometry. The pressure wave propagates along the horizontal axis of the acoustic resonator (i.e., direction along x axis in Fig.3) and it is transmitted to the acoustical space (outside the resonator) through the openings (bell and toneholes). The resonator results either in an un-flared or in a flared end (bell). The acoustic attributes of the produced sound depend on the aforementioned air column oscillations. That is the reason why it is the instrument's geometry, rather than the material that most significantly affects the produced sound [18]–[20].

Wind instruments allow the alteration of the generated pitch through various techniques and mechanisms (e.g., toneholes, slide mechanisms, by means of embouchure). In this work we consider only the use of toneholes. Open toneholes significantly affect the pressure wave propagation by shortening the effective length of the air column as the pressure wave exits the resonator at first open hole closest to the mouthpiece. Closed toneholes do not affect the resonant frequency as much, but their effect cannot be neglected [12], [21]. Fingering pattern, which is a pattern of open and/or closed toneholes, allows variations of the air column's length, leading to the production of a desired pitch. The potential register holes, which are usually located on the bottom side of the resonator opposite the toneholes, extend the frequency range modifying the air column so as higher resonance frequencies will be produced.

The reed, either single or double, which is located at the tip of the mouthpiece, is the excitation mechanism of the reed wind instruments. The player's lips abut the reed's blade(s), and the air coming from the mouth flows inside the instrument's internal cavity. The pressure difference between the player's oral cavity and the reed's channel helps to define the reed movement during excitation. The reed closes as the aforementioned pressure difference increases and opens as it decreases. When the movement mentioned above becomes periodic between two extreme positions (i.e., the reed oscillates), the volume flow entering the resonator stimulates an oscillation to the air particles inside the acoustic resonator. This oscillating flow is obtained by a feedback loop consisting of the nonlinear exciter coupled to the resonator. Researchers, throughout the last decades, have extensively studied the behavior of the nonlinear phenomena governing the operation of single-reed wind instruments [12], [15], [22].

However, double-reed wind instruments are not thoroughly studied, firstly because of the complexity of the airflow that such an excitation mechanism introduces, and secondly because there is a limited number of modern instruments of this kind. The most popular double-reed instruments in our times are the oboe, the bassoon, and the bagpipe, whose reed consists of two symmetrical [17] oscillating blades followed by a conical part that works as a conical diffuser. Some alternative approaches for the physical modeling of the double-reed musical instrument of Zournas have also been presented in the literature [23]–[26].

Although not much research on the double-reed instruments has been done, there are some studies [16], [17] [27]–[31] which focus on the double-reed and the complicated, nonlinear phenomena that govern its mechanism. Most of these works study the oboe's double-reed, but not in combination with the rest of the instrument (i.e., the resonator).

According to archeomusicology, a significant number of ancient instruments were played with a double-reed, e.g., the Greek Aulos [32]–[34] and the renaissance Rauschpfeife [35]. The Aulos of Poseidonia, dated in 5th BCE, constitutes a typical representative of the classical Greek Aulos in terms of dating, geometry, and function [36]. Therefore, its acoustic study enables us to suggest generalized indications on the sound of Aulos of the classical era. In the current work, we study the double-reed of Aulos, which geometrically differs from the modern ones purely because after the blades, instead of the conical part, there is a cylindrical backbone. Andreopoulou's work on Aulos [37] focused on the capabilities of scale reproduction but not on the instrument's simulation techniques. The current work aims to provide a more robust and detailed modeling approach than previous works. Our goal is to develop a complete digital analog of this ancient wind instrument by using physical modeling techniques. In order to do so, we modified the proposed method by Almeida *et al.* [29], who studied the oboe's reed, to fit the Aulos reed case and, later, we combined the theory for the nonlinear excitation mechanism with the digital waveguide method [9], [12], [15], [38] to simulate the physics of the resonator with its toneholes. As a result, we created a digital double-reed wind instrument model that allows the customization of the instruments' geometry, i.e., the mouthpiece's length and the resonator, the positions, the size, and the number of the toneholes and the fingering pattern. In order to demonstrate a scenario of a simple, user-friendly interface, we also created a Graphical User Interface (GUI) which accepts values for the geometrical variables, virtually demonstrates a simplified geometry of the instrument, and displays the produced signal both in time and frequency domain. This model can export the fundamental frequency and its first harmonics and therefore, we expect it to be a useful tool for archeologists and archaeomusicologists to predict the musical scale or a missing part of an instrument. It should be noted here that in this work, the effect of the instrument's material was not taken into account as, in the family of instruments simulated (i.e., wind instruments with

a cylindrical resonator), it does not significantly affect the produced sound [18]–[20]. Lastly, we compared the audio generated by our model with the recorded samples taken from the replica of Aulos of Poseidonia, physically reconstructed, by following the principles of archeomusicology [39].

The structure of the current work is as follows: first, we describe in detail the modeling for the double-read and the resonator along with the toneholes. Then, we present the implementation of the read-resonator system and the open and closed toneholes. Finally, we show the validation results based on comparing the replica’s signal vs. the signal generated by the digital modeling.

II. MODEL’S DESCRIPTION

A. THE DOUBLE-REED

As mentioned in the introduction, the sound generated by a wind musical instrument is due to the oscillating air particles that cause the pressure wave propagation along the acoustic tube. In order to study this phenomenon, we first need to simulate the excitation mechanism which triggers these oscillations. In double-reed instruments, the movement of the reed’s two blades which is caused by the alterations of pressure (i.e., the pressure inside the player’s mouth and the pressure inside the reed), is the excitation mechanism. Because of the nonlinear movement of the double-reed (as the reed rapidly closes), the airflow through it is affected by phenomena such as vortices and/or turbulent flow [17], [27], [29] which cannot easily be described by analytical expressions. In this section, we present the calculation of the difference between the mouth pressure and the pressure inside the reed according to the mouth pressure and the pressure exiting the reed (i.e., the pressure right after the reed’s conical part or backbore). This is an essential step towards the simulation of the generated sound of the wind instrument as the pressure at the end of the reed equals the one entering the instrument’s resonator, where the resonance (responsible for the sound production) is taking place.

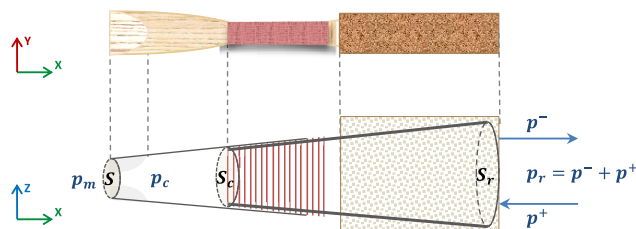


FIGURE 1. The double-reed excitation mechanism of the oboe.

Our approach of the double-reed is based on the work of Almeida *et al.* [16], [29], who studied the oboe’s double-reed excitation mechanism. In order to describe the nonlinear behavior of the double-reed in a simple model, the quasistatic regime is used to define the relationship between two variables of acoustic relevance; the pressure drop (Δp) across the reed and the volume flow (q) at its output. According to quasistatic conditions, since the quantities p and q (Fig.1)

vary sufficiently slowly in time, all time derivatives in the nonlinear characteristic relation can be neglected.

The pressure difference (Δp)_c between the mouth pressure (p_m) and the pressure inside the reed (p_c) affects the reed’s opening area (S). Both double-reed’s, the one that Almeida described [29] and the one used in this study, are inward-striking, i.e., when the mouth pressure is increased, the blades of the reed tend to close. The relation of the pressure difference and the reed’s cross-section area is given by (1)

$$(\Delta p)_c = p_m - p_c = k_S(S_0 - S) \quad (1)$$

where, S_0 is the reed’s opening at rest, and k_S is the reed’s stiffness coefficient.

Almeida *et al.* studied the double-reed’s movement by performing experimental measurements in the case of the oboe [28]. For their experiment, they use an artificial mouth which allows them to control and alternate the pressure p_m . Initially, the reed is at rest, where the pressure difference (Δp)_c equals to zero, and the reed’s opening area is at its maximum level (S_0). As the pressure p_m increases the blades are progressively closing. When the pressure difference exceeds a specific value, the reed is forced to shut ($S = 0$) rapidly. Consequently, the airflow through the reed stops, the pressure p_m suddenly increases, and the pressure p_c drops to 0. Then the mouth pressure p_m is gradually decreased. The reed remains closed until the value of p_m – and consequently the value of (Δp)_c – becomes small enough to allow for the reed to open again. Then when the reed is open, the air starts flowing again through the reed and, as a result, the mouth pressure quickly decreases and the reed pressure increases. When the pressure difference (Δp)_c becomes equal to zero, it obliges the reed to stabilize at its initial rest position. It is important to note here, that, in our simulation for simplicity reasons we assume that the mouth pressure p_m is not altered (i.e., its value is constant). This simulated constant mouth pressure (input signal) takes the value of 1 (normalized maximum) which is reached by an initial slope (corresponding to the time needed to reach the constant value). Although this simplification cannot simulate some aspects related to the player’s subtle control of the sound quality (e.g., vibrato and rapid transients), it enables the adequate approximation of the normal playing condition (i.e., production of a self-sustained steady oscillation) [40].

The volume flow (q) that enters the instrument is defined by the pressure difference (Δp)_c and the reed’s opening area, as described by Bernoulli (2).

$$q = S \sqrt{\frac{2(p_m - p_c)}{\rho}} = S \sqrt{\frac{2(\Delta p)_c}{\rho}} \quad (2)$$

where, ρ is the density of the air medium.

In the case of the oboe’s excitation mechanism, the part after the blades is conical. This geometrical feature is described by the cross-sections S_c and S_r (Fig.1) and it is considered to be a conical diffuser with a pressure recovery coefficient c_p ($0 \leq c_p \leq 1$) [29], [30]. Therefore, the total

pressure difference between mouth pressure and pressure at the exit of the reed (p_r) is:

$$p_m - p_r = (\Delta p)_c - c_p \frac{1}{2} \rho \left(\frac{q}{S_c} \right)^2 \quad (3)$$

where, S_c is the cross-section at the beginning of the conical diffuser and, assuming an ideal pressure recovery coefficient, $c_p = 1 - \frac{S_c^2}{S_r^2}$.

Combining (1) and (3), the pressure inside the reed is

$$p_c = p_r - c_p \frac{1}{2} \rho \left(\frac{q}{S_c} \right)^2 \quad (4)$$

Therefore, the pressure difference $(\Delta p)_c$ can be expressed according to the mouth pressure and the pressure at the exit of the reed, as it occurs from (1) and (4)

$$(\Delta p)_c = p_m - p_r + c_p \frac{1}{2} \rho \left(\frac{q}{S_c} \right)^2 \quad (5)$$

Ancient double-reeds (Fig.2), on the other hand, geometrically differ from modern ones. The main difference is that after the blades, instead of a conical diffuser, there is a cylindrical part, called the reed's backbore, with an inner diameter equal to the inner diameter of the instrument's resonator.

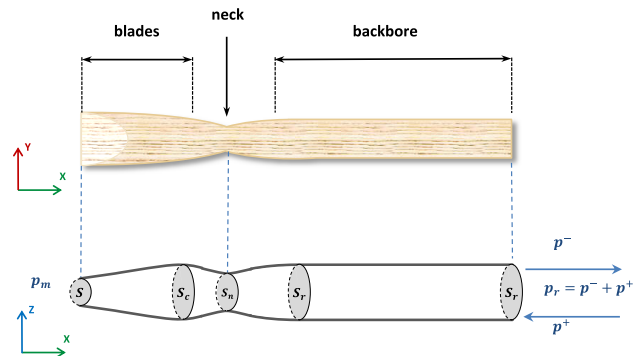


FIGURE 2. Ancient double-reed with cylindrical backbore.

In the case of the double-reed with a cylindrical backbore, there is a neck located between the blades and the backbore. As shown in Fig.2, S_c is the section area before the reed's neck, S_n is the section area of the neck and S_r is the section area of the backbore.

Applying Bernoulli's law between S_c and S_n and between S_n and S_r respectively, we get:

$$p_c + \frac{1}{2} \rho \frac{q^2}{S_c^2} = p_n + \frac{1}{2} \rho \frac{q^2}{S_n^2} \quad (6)$$

$$p_n + \frac{1}{2} \rho \frac{q^2}{S_n^2} = p_r + \frac{1}{2} \rho \frac{q^2}{S_r^2} \quad (7)$$

The combination of the above relations gives:

$$p_r = p_c + \left(1 - \frac{S_c^2}{S_r^2} \right) \frac{1}{2} \rho \frac{q^2}{S_c^2} \quad (8)$$

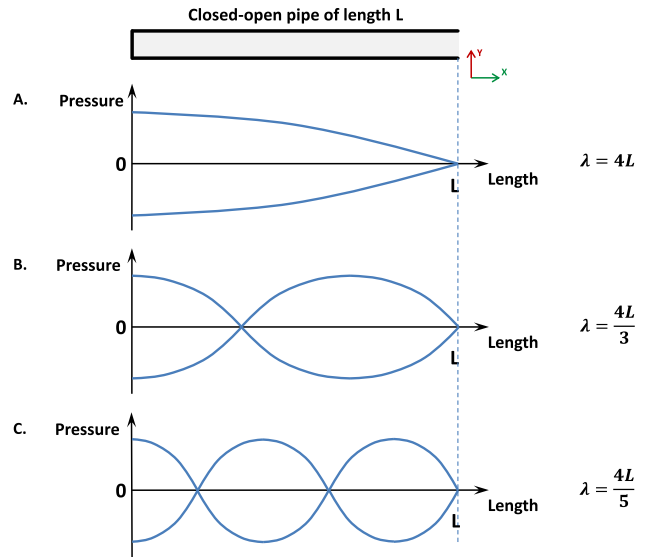


FIGURE 3. Harmonics of a closed-open pipe in three different wavelengths: A. Four times the length of the pipe ($4L$) B. Four thirds the length of the pipe ($4L/3$) and C. Four fifths the length of the pipe ($4L/5$).

As in oboe's reed, we can set the constant $c_p = 1 - \frac{S_c^2}{S_r^2}$ and, since in the ancient double-reed's case $S_n \approx S_r$, then we conclude that $c_p = 0$ and thus, according to (8), $p_r = p_c$ i.e. the pressure inside the reed's blades equals the pressure entering the instrument's bore.

In our simulation, we consider a double-reed with such a cylindrical backbore (Fig.2), so the pressure difference $(\Delta p)_c$ results from (5) as

$$(\Delta p)_c = p_m - p_r \quad (9)$$

B. THE RESONATOR

The airflow coming from the reed enters the instrument's bore and forces the air particles inside the resonator to vibrate. Assuming a simple closed-open tube without tone-holes, the pressure waves travel along the tube and partially come back every time they reflect at each end, forming a standing wave inside the resonator. When the waves reach the open end, they are reflected back with a phase change of π , while, at the closed end, the waves are reflected back without phase change [18]. In the physics theory governing reed instruments, the resonator's end, where the reed is attached, is considered to be closed because the reed's opening area is much smaller than the resonator's diameter. However, the other end is open to the outside air. Therefore, Aulos' resonator (a cylindrical wind reed instrument) behaves as a closed-open pipe, which produces only the odd harmonics with respect to the fundamental produced frequency. At the closed end, there is a pressure antinode (i.e., the sound pressure becomes maximum), and the displacement of the air particles equals zero. At the open end, there is a pressure node where the sound pressure equals zero (the pressure is approximately atmospheric), and the displacement of the oscillating air particles becomes maximum. Fig.3 A, B, and C show few examples of pressure waves with wavelengths of

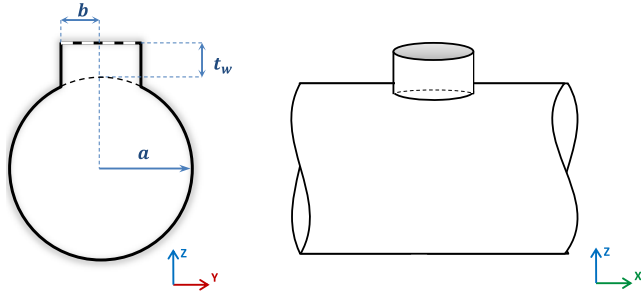


FIGURE 4. The geometry of the tonehole.

$4L$, $4L/3$, and $4L/5$, respectively, which can be formed inside a cylindrical closed-open pipe of length L .

C. THE TONEHOLES

The toneholes are located in the resonator part of the wind instrument allowing variations of the air column’s effective length corresponding to the fingering pattern [21]. The transmission of the pressure waves happens at the closest to the mouthpiece open hole, which acts as an unflared end. The toneholes are cylindrical tubes of radius b , which are attached to the resonator as shown in Fig.4, and they define the pitching of the wind instrument. Setting as a the cross-sectional area of the resonator and t_w the shortest height of the tonehole’s chimney, the tonehole height t is approximated [12] by

$$t = t_w + \frac{1}{8} \frac{b}{a} \left[1 + 0.172 \left(\frac{b}{a} \right)^2 \right] \quad (10)$$

III. IMPLEMENTATION

A. THE RESONATOR

The resonator is modeled as a one-dimensional digital waveguide by using delay lines [12], [15], [38]. The delay line is an elementary functional unit used to simulate traveling wave propagation and constitutes the fundamental building block of digital waveguide synthesis. The sum of the traveling waves at a point gives the total power at that point in the waveguide. The pressure p_r exiting the reed equals the pressure entering the instrument’s resonator because the resonator’s cross-sectional area equals the one at the reed’s exit (Fig.5). Considering p^+ as the left-going and p^- as the right-going traveling wave (Fig.2), the total pressure inside the resonator is:

$$p_r = p^+ + p^- \quad (11)$$

The relation between the right-going pressure p^- and the left-going pressure p^+ , can be expressed according to a reflection coefficient (r , (12)), which concerns the reflection at the closed end of the bore. For simplicity reasons and because of the symmetrical displacement of the reed’s blades in the X-axis [16], [17], we use the reflection coefficient of a single reed as it is described in [15]. When the mouth pressure exceeds the pressure inside the reed, the reed closes,

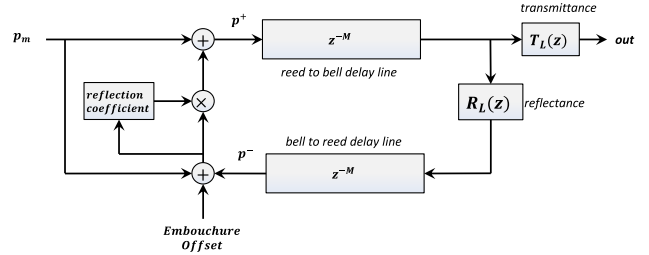


FIGURE 5. Block diagram of the Aulos’ digital waveguide model.

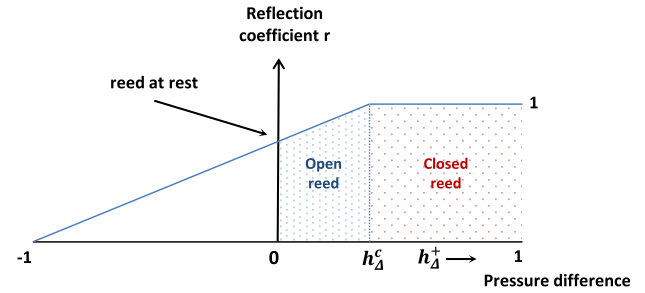


FIGURE 6. Reflection coefficient of the reed.

and the reflection coefficient equals 1. When the reed opening reaches its maximum value, the reflection coefficient equals 0.

$$p^- = rp^+ + \frac{1-r}{2} p_m \quad (12)$$

Smith [15] suggests the reflection coefficient function (13) depicted in Fig.6, which introduces the nonlinearity, for $h_\Delta^+ \triangleq \frac{p_m}{2} - p_b^+$ and $m = \frac{1}{h_\Delta^c + 1}$. The point h_Δ^c is the smallest pressure difference giving reed closure.

$$r = \begin{cases} 1 - m(h_\Delta^c - h_\Delta^+), & -1 \leq h_\Delta^+ \leq h_\Delta^c \\ 1, & h_\Delta^c \leq h_\Delta^+ \leq 1 \end{cases} \quad (13)$$

B. THE REED-RESONATOR SYSTEM

The combination of (5), (11), and (12) gives the relation between the pressure difference $(\Delta p)_c$ and the mouth pressure, the reflection coefficient and the left-going resonator pressure p^+ .

$$(\Delta p)_c = \frac{(1+r) \left(\frac{1}{2} p_m - p^+ \right)}{1 - c_p \left(\frac{S}{S_c} \right)^2}$$

for $Aulos(c_p \approx 0) \rightarrow (\Delta p)_c = (1+r) \left(\frac{1}{2} p_m - p^+ \right) \quad (14)$

Therefore, the total pressure p_r inside the resonator now occurs from (3).

$$p_r = p_m - (\Delta p)_c + c_p \frac{1}{2} \rho \left(\frac{q}{S_c} \right)^2$$

for $Aulos(c_p \approx 0) \rightarrow p_r = p_m - (\Delta p)_c \quad (15)$

C. TONEHOLES

The effect of the tonehole, either open or closed, can be represented as a lumped circuit, symmetric T transmission line model (Fig.7) with shunt impedance (Z_s) and series impedances (Z_a) [21]. The shunt impedance corresponds to the standing wave inside the resonator, directly under the tonehole. In contrast, the series impedance is related to the pressure standing wave along the propagation axis at the place of the tonehole.

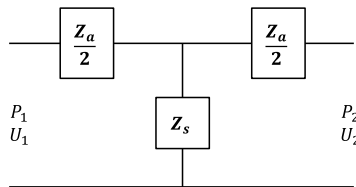


FIGURE 7. T -transmission line model of the tonehole.

In the case of a pressure node at the tonehole junction, the volume flow (U) is symmetric across the junction. If there is a pressure anti-node at the tonehole junction, the symmetry across the junction is related to the pressure (P).

The characteristic impedance of the instrument's resonator is

$$R_0 = \frac{\rho c}{\pi a^2} \quad (16)$$

where ρ is the air density, and c is the speed of sound in the propagation medium (i.e., air).

According to Keefe [21], the lumped circuit, assuming that $|Z_a/Z_s| \ll 1$, is represented in (17), where the values of Z_s and Z_a depend on the status of the hole (open or closed)

$$\begin{bmatrix} P_1 \\ U_1 \end{bmatrix} = \begin{bmatrix} 1 & Z_a \\ Z_s^{-1} & 1 \end{bmatrix} \begin{bmatrix} P_2 \\ U_2 \end{bmatrix} \quad (17)$$

The reflectance and the transmittance [12] of the tonehole are given by

$$r = \frac{Z_a Z_s - R_0^2}{Z_a Z_s + 2R_0 Z_s + R_0^2} \quad (18)$$

$$t = \frac{2R_0 Z_s}{Z_a Z_s + 2R_0 Z_s + R_0^2} \quad (19)$$

1) OPEN TONEHOLES

The series impedance for an open-hole represents a negative length correction to the resonator, and the predicted value has a similar order of magnitude as the predicted closed-hole series impedance. The shunt impedance of an open-hole in the absence of dissipation and with negligible radiation is an inertance that involves both inner and outer length corrections as well as the tonehole's chimney height.

An open tonehole's specific resistance ξ_e accounts for visco-thermal losses at the walls of the tonehole. Considering r_c as the radius of the resonator's curvature, the specific resistance is given by

$$\xi_e = 0.25(kb)^2 + \alpha t + \frac{1}{4} k d_v \ln \left(\frac{2b}{r_c} \right) \quad (20)$$

where $k = \omega/c$ is the wavenumber, α can be calculated by (21), and it is described in the literature as either the attenuation coefficient [41] or the real part of the propagation wavenumber [42], and $d_v = \sqrt{2\eta/(\rho\omega)}$ is the viscous boundary layer thickness in relation with the air's shear viscosity η .

$$\alpha = \frac{3 \cdot 10^{-5}}{b} \sqrt{\frac{\omega}{2\pi}} \quad (21)$$

The effective length of an open tonehole is given by (22).

$$t_e = \frac{k^{-1} \tan(kt) + b \left[1.4 - 0.58 \left(\frac{b}{a} \right)^2 \right]}{1 - 0.61kb \tan(kt)} \quad (22)$$

The open tonehole (o) series equivalent length [21] is

$$t_a^{(o)} = \frac{0.47b \left(\frac{b}{a} \right)^4}{\tanh \left(1.84 \frac{t}{b} \right) + 0.62 \left(\frac{b}{a} \right)^2 + 0.64 \frac{b}{a}} \quad (23)$$

The series impedance $Z_a^{(o)}$ and the shunt impedance $Z_s^{(o)}$ of the T -transmission line model for an open tonehole [21] are given by

$$Z_a^{(o)} = -jR_0 \left(\frac{a}{b} \right)^2 k t_a^{(o)} \quad (24)$$

$$Z_s^{(o)} = R_0 \left(\frac{a}{b} \right)^2 (j k t_e + \xi_e) \quad (25)$$

2) CLOSED TONEHOLES

The shunt impedance for a closed tonehole in the low-frequency limit is an acoustic compliance, whose volume equals the closed-hole volume. The series impedance for a closed tonehole may be written as a negative length correction; that is, the presence of a closed-tonehole at a pressure node is equivalent to a reduction in the main resonator length in the vicinity of the tonehole.

The closed tonehole (c) series equivalent length [21] is

$$t_a^{(c)} = \frac{0.47b \left(\frac{b}{a} \right)^4}{\coth \left(1.84 \frac{t}{b} \right) + 0.62 \left(\frac{b}{a} \right)^2 + 0.64 \frac{b}{a}} \quad (26)$$

The series impedance $Z_a^{(c)}$ and the shunt impedance $Z_s^{(c)}$ of the T -transmission line model for a closed tonehole [21] are given by

$$Z_a^{(c)} = -jR_0 \left(\frac{a}{b} \right)^2 k t_a^{(c)} \quad (27)$$

$$Z_s^{(c)} = -jR_0 \left(\frac{a}{b} \right)^2 \cot(kt) \quad (28)$$

D. IMPLEMENTATION OF THE PHYSICAL MODELING

Fig.8 presents the Graphical User Interface of the application we have developed in MATLAB 2020b to implement the physical modeling calculations described above. For the example shown in Fig.8, the parameters are set according to the ancient Greek Aulos of Poseidonia [36]. The user sets Aulos main physical parameters, then the fingering (open/closed toneholes) and the geometrical features of the

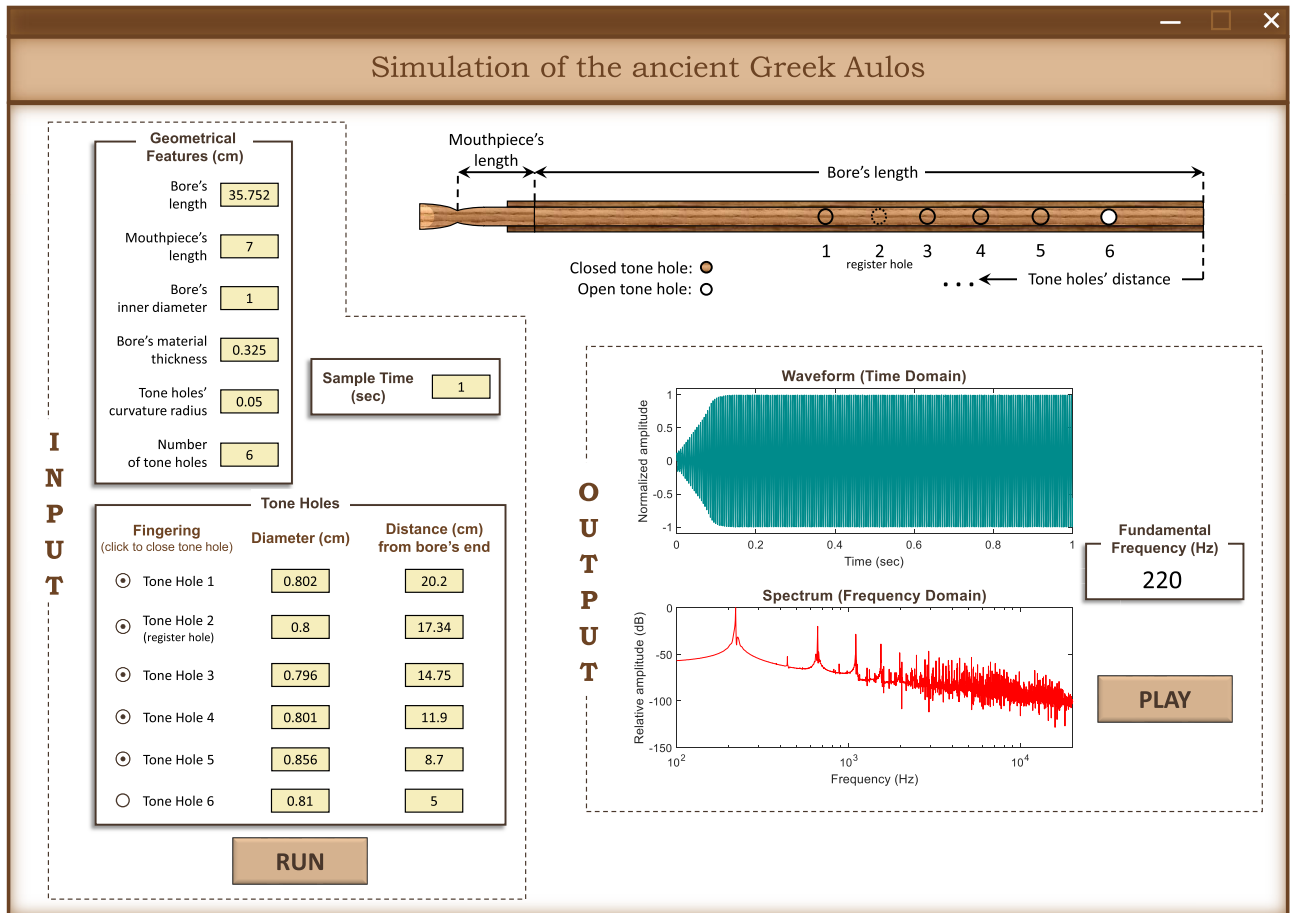


FIGURE 8. Graphical user interface for implementing the physical modeling of Aulos showing the model's input parameters and the results as playable audio and its plots in the time and frequency domain. The parameters are set according to the geometrical features of the Aulos of Poseidonia.

toneholes. An open hole is depicted as a white circle (in the example shown in Fig.8 only the sixth tonehole is open). Then the user hits the “RUN” button to start the calculations of the physical modeling. As a result, an audio file is produced (the user can listen to it by hitting the “Play” button), along with the plots of its signal in time and frequency domain.

IV. VALIDATION

In order to evaluate our physical modeling approach described above, we coded the model using MATLAB 2020b and compared its audio output signals (Fig.9b) with the recorded signals (Fig.9a) from the replica instrument of Aulos of Poseidonia.⁵ Since the double reed instrument Aulos can be described as a closed-open pipe and therefore it is

⁵This particular replica of the Poseidonia aulos was physically reconstructed at the premises of the Speech and Accessibility Laboratory of the National and Kapodistrian University of Athens, Department of Informatics and Telecommunications, on the course of the HERMES: “Towards a training music archaeology project on the reconstruction and use of ancient Hellenic Musical Instruments” project implementation [4]. This specific reconstruction is based on detailed images, measurements, and designs of the original find provided by Reichlin-Moser, Paul J. & Barbara [2013] in *Der Paestum Aulós aus der Tomba del Prete*. (Illustration by Verena Pavoni, Visuelle Gestaltung: Ulrich Schuwey)

producing only the odd harmonics [18], our comparison is focusing, in the frequency domain, on the fundamental frequencies and their odd harmonics. In some of the recorded signals, even harmonics were present, as can be seen in Fig.9a₂. This could be due to the factors, for simplification reasons, not considered in our model such as the reed's saliva and the shape of the main resonator not being perfectly cylindrical. Nevertheless, the study of this phenomenon is beyond the scope of this work.

We recorded the low pipe replica of the Aulos of Poseidonia with the musician (Georgios Barbarekos) performing the seven fingerings to reproduce a scale. The microphones were placed approximately 1m away from the instrument off axis from the instrument's bell and the musician played in piano level every note once. Fig.9 shows the case of one open tonehole for both the recording (Fig.9a) and the physical model (Fig.9b). Their signals are shown in the time and frequency (using Fourier transformation of 1 second recorded signal) domain. The recordings took place at the studio of the Laboratory of Music Acoustics and Technology, Department of Music Studies, National and Kapodistrian University of Athens, on March 4th, 2021. The equipment used: Microphone Preamplifier: Millennia HV-3D, A/D Converter:

RME ADI A8 DS, Microphones: Neumann km184, and stereo pair of Beyerdynamic M130 (Mid-Side technique).

We first compare the time domain characteristics of the recorded (Fig.9a₁) and the simulated (Fig.9b₁) signal by studying their dynamic temporal envelope. We observe that our model simulates adequately the temporal characteristics of the recording. The recorded and generated signals both need the same amount of time to reach their steady-state oscillation (i.e., attack of approx. 100msec followed by a prolonged sustain), marked with a yellow dashed line in Fig.9a₁ and Fig.9b₁. This is expected due to the inherent properties of the digital waveguides which adequately transform the signal propagation in the continuous space of the physical instrument into the discrete space of the virtual instrument. Considering the above, similar inputs (in our case a constant mouth pressure) for both the physical and the virtual instrument result to a correspondingly similar attack. Taking into account that the time introduced into the model is related to the adopted excitation method [12] is the first validation of our double-reed implementation. The prolonged sustain is due to the continuous existence of the excitation force (i.e., the constant air supply from the player).

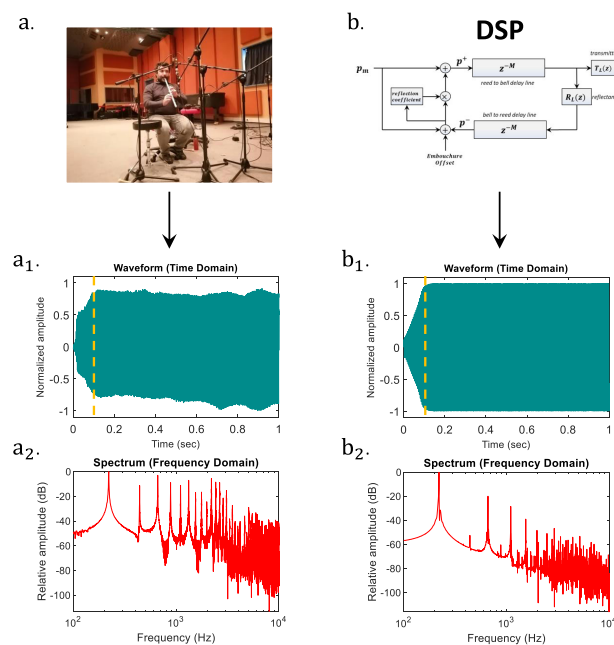


FIGURE 9. Signal comparison of aulos: The recorded signal of the replica (a) vs. the generated signal by the digitally implementation of the physical modeling of Aulos using MATLAB 2020b (b), along with their plots in the time (a₁, b₁) and frequency (a₂, b₂) domain.

Secondly, we compare the two signals in the frequency domain. In order to study the timbre characteristics, we consider the fundamental and the three first harmonics (Table 1). The difference in cents was calculated using the formula $1200 \log_2 \left(\frac{a}{b} \right)$ where a and b are the frequencies (Hz) being compared. The musician during the recordings reproduced the scale that the instrument naturally generates according to its geometry and to the available reeds. This resulted

TABLE 1. Comparison of the signals from our physical model (PM) vs. the corresponding Aulos of Poseidonia’s low pipe replica recordings (Rec) (C: Closed tonehole, O: Open tonehole, Dev: Deviation in cents, Fundam.: Fundamental, OT: Overtone).

Fingering		Timbre Characteristics			
		Partial			
		Fundam.	1 st OT	2 nd OT	3 rd OT
CCCCCC	PM (Hz)	206	617	1028	1439
	Rec (Hz)	205	615	1026	1439
	Dev. (c)	8	6	3	0
CCCCCO	PM (Hz)	220	660	1099	1539
	Rec (Hz)	221	662	1103	1543
	Dev. (c)	-8	-5	-6	-4
CCCCOO	PM (Hz)	241	722	1203	1684
	Rec (Hz)	241	723	1202	1684
	Dev. (c)	0	-2	1	0
CCCOOO	PM (Hz)	264	792	1321	1849
	Rec (Hz)	264	793	1320	1849
	Dev. (c)	0	-2	1	0
CCOOOO	PM (Hz)	291	875	1459	2029
	Rec (Hz)	290	871	1456	2028
	Dev. (c)	6	8	4	1
COOOOO	PM (Hz)	323	968	1613	2258
	Rec (Hz)	320	963	1610	2248
	Dev. (c)	16	9	3	8
OOOOOO	PM (Hz)	360	1081	1802	2523
	Rec (Hz)	359	1077	1797	2517
	Dev. (c)	5	6	5	4
Rounded average of absolute Dev. (c)		6	5	3	2

in a diatonic scale the tonic center of which is defined by the third fingering pattern, forming with the 6th and 7th fingering patterns the approximately pure intervals of the fourth and fifth, respectively. In the case of four open toneholes, the fundamental frequency of the recorded signal is 320Hz, and the simulated one is 323Hz deviating by 3Hz, which is translated to -16 cents. This mismatch is the most remarkable frequency difference of all the fingerings we compared, and it is still slightly above Just Noticeable Difference (JND) [43], [44]. In more detail, the absolute deviation in cents of the fundamental frequencies shows an average deviation of 6 cents and a standard deviation of ± 5 cents. The first harmonics show an average deviation of 5 cents and a standard deviation of ± 3 cents; the second harmonics show an average deviation of 8 cents and a standard deviation of ± 8 cents. The third harmonic shows an average deviation of 2 cents and a standard deviation of ± 3 cents. All the above results can be considered perceptually insignificant as they are well below the JND. Inharmonicity (i.e., the deviation of the overtone frequencies from the perfect integer multiples of the fundamental frequency), which is a factor that defines the

TABLE 2. Inharmonicity of the signals from our physical model (PM) vs. the corresponding Aulos of Poseidonia's low pipe replica recordings (Rec) (C: Closed tonehole, O: Open tonehole, IH: Inharmonicity in cents, Diff.: Difference between the inharmonicity of PM and the inharmonicity of Rec in cents, OT: Overtone, abs: Absolute, Avg: Average).

Fingering	IH (c)	1 st OT	2 nd OT	3 rd OT	Rounded Avg of abs IH per Fingering
CCCCC	PM	-3	-3	-4	3
	Rec	0	2	5	2
	Diff.	-3	-5	-9	
CCCCO	PM	0	-2	-1	1
	Rec	-3	-3	-4	3
	Diff.	3	1	3	
CCCCOO	PM	-2	-3	-3	3
	Rec	0	-4	-3	2
	Diff.	-2	1	0	
CCOOO	PM	0	1	1	1
	Rec	2	0	1	1
	Diff.	-2	1	0	
CCOOOO	PM	4	5	-7	5
	Rec	2	7	-2	4
	Diff.	2	-2	-5	
COOOO	PM	-2	-2	-2	2
	Rec	5	11	6	7
	Diff.	-7	-13	-8	
OOOOO	PM	2	2	2	2
	Rec	0	2	3	2
	Diff.	2	0	-1	
Rounded Avg of abs IH per OT	PM	2	3	3	
	Rec	2	4	3	

timbre, is similar for both the recorded and the synthesized signal (approx. 3 cents in average), see Table 2. Moreover, the total inharmonicity (calculated as the average absolute deviation for the first three overtones, demonstrated in the last column of Table 2) differentiates less than 2 cents for both the recorded and the synthesized signal in all fingerings, except for the COOOO which differs by 5 cents.

The microphones in the recordings were placed 1m away from the instrument and the output signal from our model was in the beginning of the mouthpiece (see Fig.8). The effect of the bell is to radiate out of the instrument the high frequencies and to reflect back the low frequencies. This reflectance can be modeled as a low-pass filter [12]. Thus, the signal generated by our model (where the output is positioned inside the resonator) compared with the relative recording (microphone as well as a potential listener positioned outside the resonator) is missing energy in the high frequencies.

V. CONCLUSION

In this investigation, we presented a digital model of Aulos, a double-reed wind instrument, implemented with physical

modeling techniques. We considered two parts of the instrument in order to describe and simulate the physical phenomena (the excitation mechanism and the resonator with toneholes). Aulos excitation mechanism is the double-reed, consisting of two symmetrical blades followed by a cylindrical backbore in contrast with the conical backbore of the recently used double-reeds such as the oboe's one. The nonlinear behavior of the double-reed is described by using quasistatic regimes defining the relation between the pressure difference and the volume flow across the reed. We used a one-dimensional digital waveguide to simulate the instrument's resonator simulating the pressure traveling wave propagation and the air particles' oscillation inside the resonator. The effect of the open and/or closed toneholes is modeled with respect to their impedances as a lumped T-transmission line circuit.

The comparison of the signal recorded by the replica of Aulos of Poseidonia, built in our lab, with the signal generated by the relevant physical modeling digital implementation of the instrument showed good agreement, especially in the frequency domain. In the time domain, our model simulates temporal characteristics of the recording, but further improvements could be made by applying an Attack, Decay, Sustain, Release (ADSR) envelope. In the frequency domain for a scale (seven notes), the fundamental frequencies and the three first harmonics of the signals differ only 6, 5, 3, and 2 cents on average, respectively, which is below the Just Noticeable Difference threshold. Further, the resonant frequencies in both signals only slightly differentiate from the odd multiples of the corresponding fundamental, as expected by the theory, and their total average absolute inharmonicity is approximately 3 cents for both of them.

Moreover, by clearly describing the physical phenomena, we expect to inspire researchers to: a) improve the current model by resolving the constrain of the calculated pressure point been inside the resonator and the absence of the even harmonics (as per the theory of a closed-open pipe), b) describe musical instruments as acoustic metamaterials like various apparatus are used in other fields of acoustics [45], [46] and, c) by knowing the acoustics of ancient theatres [47], [48], making them virtually sound again as they use to in their natural auditory space.

ACKNOWLEDGMENT

The authors would like to thank the musician Georgios Barbarekos for playing Aulos of Poseidonia.

REFERENCES

- [1] A. Allen and N. Raghuvanshi, "Aerophones in flatland: Interactive wave simulation of wind instruments," *ACM Trans. Grap.*, vol. 34, no. 4, p. 134, 2015, doi: [10.1145/2767001](https://doi.org/10.1145/2767001).
- [2] K. Bakogiannis, S. Polychronopoulos, D. Marini, C. Terzes, and G. T. Kouroupetoglou, "ENTROTUNER: A computational method adopting the Musician's interaction with the instrument to estimate its tuning," *IEEE Access*, vol. 8, pp. 53185–53195, 2020, doi: [10.1109/ACCESS.2020.2981007](https://doi.org/10.1109/ACCESS.2020.2981007).
- [3] S. Bilbao, "Direct simulation for wind instrument synthesis," in *Proc. 11th Int. Digit. Audio Effects Conf.*, Espoo, Finland, Sep. 2008, pp. 145–152. [Online]. Available: <https://bit.ly/3vIumuP>

- [4] A. Hunt, M. M. Wanderley, and M. Paradis, "The importance of parameter mapping in electronic instrument design," *J. New Music Res.*, vol. 32, no. 4, pp. 429–440, Dec. 2003, doi: [10.1076/jnmr.32.4.429.18853](https://doi.org/10.1076/jnmr.32.4.429.18853).
- [5] N. Schnell and M. Battier, "Introducing composed instruments, technical and musicological implications," in *Proc. Conf. New Interface Musical Expression*, 2002, pp. 1–5. [Online]. Available: <https://bit.ly/3cOFbMD>
- [6] F. Avanzini, S. Canazza, G. De Poli, C. Fantozzi, E. Micheloni, N. Pretto, R. Antonio, S. Gasparotto, and G. Salemi, "Virtual reconstruction of an ancient Greek pan flute," in *Proc. Int. Conf. Sound Music Comput. (SMC)*, Sep. 2016, pp. 41–46. [Online]. Available: <https://bit.ly/3bOPYxX>
- [7] Z. Sun, A. Rodà, E. Whiting, E. Faresin, and G. Salemi, "3D virtual reconstruction and sound simulation of an ancient Roman brass musical instrument," in *Proc. Int. Conf. Hum.-Comput. Interact.*, Cham, Switzerland: Springer, Jul. 2020, pp. 267–280, doi: [10.1007/978-3-030-50267-6](https://doi.org/10.1007/978-3-030-50267-6).
- [8] R. Rabenstein and L. Trautmann, "Digital sound synthesis by physical modelling," in *Proc. 2nd Int. Symp. Image Signal Process. Anal. Conjoint 23rd Int. Conf. Inf. Technol. Interface (ISPA)*, Jun. 2001, pp. 12–23.
- [9] J. O. Smith, III, "Physical modeling using digital waveguides," *Comput. Music J.*, vol. 16, no. 4, pp. 74–91, 1992, doi: [10.2307/3680470](https://doi.org/10.2307/3680470).
- [10] V. Välimäki and T. Takala, "Virtual musical instruments—Natural sound using physical models," *Organ. Sound*, vol. 1, no. 2, p. 75, 1996, doi: [10.1017/S1355771896000039](https://doi.org/10.1017/S1355771896000039).
- [11] J.-P. Dalmont, J. Gilbert, and S. Ollivier, "Nonlinear characteristics of single-reed instruments: Quasistatic volume flow and reed opening measurements," *J. Acoust. Soc. Amer.*, vol. 114, no. 4, pp. 2253–2262, Oct. 2003, doi: [10.1121/1.1603235](https://doi.org/10.1121/1.1603235).
- [12] G. Scavone, "An acoustic analysis of single-reed woodwind instruments with an emphasis on design and performance issues and digital waveguide modeling techniques," Ph.D. dissertation, Dept. Music, Stanford Univ., Stanford, CA, USA, 1997. [Online]. Available: <https://bit.ly/38WZCfQ>
- [13] P. Guillemain, J. Kergomard, and T. Voïnier, "Real-time synthesis of clarinet-like instruments using digital impedance models," *J. Acoust. Soc. Amer.*, vol. 118, no. 1, pp. 483–494, Jul. 2005, doi: [10.1121/1.1937507](https://doi.org/10.1121/1.1937507).
- [14] M. E. McIntyre, R. T. Schumacher, and J. Woodhouse, "On the oscillations of musical instruments," *J. Acoust. Soc. Amer.*, vol. 74, no. 5, pp. 1325–1345, 1983, doi: [10.1121/1.39015](https://doi.org/10.1121/1.39015).
- [15] J. O. Smith III, "Principles of digital waveguide models of musical instruments," in *Applications of Digital Signal Processing to Audio and Acoustics*, vol. 437. Boston, MA, USA: Springer, 2002, pp. 417–466, doi: [10.1007/0-306-47042-X_10](https://doi.org/10.1007/0-306-47042-X_10).
- [16] A. Almeida, C. Vergez, and R. Caussé, "Experimental investigations on double reed quasi-static behavior," in *Proc. Int. Congr. Acoust.*, 2004, pp. 1229–1232. [Online]. Available: <https://bit.ly/2Qn3fpd>
- [17] C. Vergez, A. Almeida, R. Causse, and X. Rodet, "Toward a simple physical model of double-reed musical instruments: Influence of aerodynamical losses in the embouchure on the coupling between the reed and the bore of the resonator," *Acta Acustica United With Acustica*, vol. 89, no. 6, pp. 964–973, 2003. [Online]. Available: <https://bit.ly/3vEq69>
- [18] N. H. Fletcher and T. D. Rossing, "Materials for musical instruments," in *The Physics of Musical Instruments*. New York, NY, USA: Springer, 1998, pp. 711–734, doi: [10.1007/978-1-4612-2980-3](https://doi.org/10.1007/978-1-4612-2980-3).
- [19] T. R. Moore, B. R. Gorman, M. Rokni, W. Kausel, and V. Chatziioannou, "Axial vibrations of brass wind instrument bells and their acoustical influence: Experiments," *J. Acoust. Soc. Amer.*, vol. 138, no. 2, pp. 1233–1240, Aug. 2015, doi: [10.1121/1.4928138](https://doi.org/10.1121/1.4928138).
- [20] M. Paquier, E. Hendrickx, and R. Jeannin, "Effect of wood on the sound of oboe as simulated by the chanter of a 16-inch French bagpipe," *Appl. Acoust.*, vol. 103, pp. 47–53, Feb. 2016, doi: [10.1016/j.apacoust.2015.10.008](https://doi.org/10.1016/j.apacoust.2015.10.008).
- [21] D. H. Keefe, "Theory of the single woodwind tone hole," *J. Acoust. Soc. Amer.*, vol. 72, no. 3, pp. 676–687, Sep. 1982, doi: [10.1121/1.388248](https://doi.org/10.1121/1.388248).
- [22] J. O. Smith III, "Efficient simulation of the reed-bore and bow-string mechanisms," in *Proc. Int. Comput. Music Conf.*, 1986, pp. 275–280.
- [23] P. Tzevelekos and G. Kouroupetroglou, "Acoustical analysis of woodwind musical instruments for virtual instrument implementation by physical modeling," in *Proc. Conf. Acoust.*, 2004, pp. 49–60. [Online]. Available: <https://bit.ly/3bYVuhx>
- [24] P. Tzevelekos, T. Perperis, V. Kyritsi, and G. Kouroupetroglou, "A component-based framework for the development of virtual musical instruments based on physical modeling," in *Proc. 4th Sound Music Comput. Conf.*, 2007, pp. 30–37. [Online]. Available: <https://bit.ly/30Z4bIG>
- [25] A. Kontogeorgakopoulos, P. Tzevelekos, and G. Kouroupetroglou, "Using the CORDIS-ANIMA formalism for the physical modeling of the Greek Zournas shawm," in *Proc. Int. Comput. Music Conf.*, 2008, pp. 395–398. [Online]. Available: <https://bit.ly/3rb0q7v>
- [26] P. Tzevelekos, A. Georgaki, and G. Kouroupetroglou, "HERON: A zournas digital virtual musical instrument," in *Proc. 3rd Int. Conf. Digit. Interact. Media Entertainment Arts (DIMEA)*, 2008, pp. 352–359, doi: [10.1145/1413634.1413698](https://doi.org/10.1145/1413634.1413698).
- [27] A. Almeida, C. Vergez, R. Caussé, and X. Rodet, "Experimental research on double reed physical properties," in *Proc. Stockholm Music Acoust. Conf.*, R. Bresin, Ed. Stockholm, Sweden: KTH, 2003, pp. 243–246. [Online]. Available: <https://bit.ly/38Y0y1X>
- [28] A. Almeida, C. Vergez, R. Caussé, and X. Rodet, "Physical model of an oboe: Comparison with experiments," in *Proc. Int. Symp. Musical Acoust.* 2004, p. 1. [Online]. Available: <https://bit.ly/3eVnmoB>
- [29] A. Almeida, C. Vergez, and R. Caussé, "Quasistatic nonlinear characteristics of double-reed instruments," *J. Acoust. Soc. Amer.*, vol. 121, no. 1, pp. 536–546, Jan. 2007, doi: [10.1121/1.2390668](https://doi.org/10.1121/1.2390668).
- [30] A. Almeida, "The physics of double-reed wind instruments and its application to sound synthesis," Ph.D. dissertation, IRCAM, Sound Anal. Synth. Team, Paris VI Univ., Paris, France, 2006.
- [31] P. Guillemain, "A digital synthesis model of double-reed wind instruments," *EURASIP J. Adv. Signal Process.*, vol. 2004, no. 7, pp. 990–1000, Dec. 2004, doi: [10.1155/S110865704402194](https://doi.org/10.1155/S110865704402194).
- [32] S. Hagel, "Calculating aulos: The Louvre Aulos scale," *Studien Zur Musikarchäologie*, vol. 4, no. 14, pp. 373–390, 2004.
- [33] S. Hagel, "Better understanding the Louvre Aulos," *Studien Zur Musikarchäologie*, vol. 9, pp. 131–142, Jan. 2014. [Online]. Available: <https://bit.ly/3eVcLto>
- [34] M. L. West, *Ancient Greek Music*. Oxford, U.K.: Clarendon Press, 1992.
- [35] A. Hirschberg, X. Pelorson, and J. Gilbert, "Aeroacoustics of musical instruments," *Meccanica*, vol. 31, no. 2, pp. 131–141, Apr. 1996, doi: [10.1007/BF00426256](https://doi.org/10.1007/BF00426256).
- [36] S. Psaroudakēs, "The Aulos of Poseidōnia," in *Musica, Culti e Riti Nell'Occidente Greco*. Pisa, Roma: Istituti Editoriali e Poligrafici Internazionali, 2014, pp. 117–129.
- [37] A. Andreopoulou and A. Roginska, "Computer-aided estimation of the athenian Agora Aulos scales based on physical modeling," in *Proc. AES 133rd Conv.*, San Francisco, CA, USA, 2012, pp. 474–483. [Online]. Available: <https://bit.ly/3tzLnFQ>
- [38] G. Scavone, "Delay-lines and digital waveguides," in *Springer Handbook Systematic Musicology*. Berlin, Germany: Springer, 2018, pp. 259–272, doi: [10.1007/978-3-662-55004-5_13](https://doi.org/10.1007/978-3-662-55004-5_13).
- [39] S. Psaroudakēs, "How the present can inform the past, part i ancient and modern analogues as supplementary evidence in reconstructing an ancient instrument," *Greek Roman Musical Stud.*, vol. 8, no. 2, pp. 217–229, Aug. 2020, doi: [10.1163/22129758-BJA10006](https://doi.org/10.1163/22129758-BJA10006).
- [40] B. Fabre, J. Gilbert, and A. Hirschberg, "Modeling of wind instruments," in *Springer Handbook Systematic Musicology*. Berlin, Germany: Springer, 2018, pp. 121–139, doi: [10.1007/978-3-662-55004-5_7](https://doi.org/10.1007/978-3-662-55004-5_7).
- [41] V. Välimäki, M. Karjalainen, and T. I. Laakso, "Modeling of woodwind bores with finger holes," in *Proc. Int. Comput. Music Conf.*, 1993, pp. 32–39.
- [42] D. H. Keefe, "Woodwind air column models," *J. Acoust. Soc. Amer.*, vol. 88, no. 1, pp. 35–51, Jul. 1990, doi: [10.1121/1.399911](https://doi.org/10.1121/1.399911).
- [43] B. Kollmeier, T. Brand, and B. Meyer, "Perception of speech and sound," in *Springer Handbook of Speech Processing*, J. Benesty, M. M. Sondhi, and Y. Huang, Eds. Berlin, Germany: Springer, 2008, pp. 61–82, doi: [10.1007/978-3-540-49127-9_4](https://doi.org/10.1007/978-3-540-49127-9_4).
- [44] M. Long, *Architectural Acoustics*. Amsterdam, The Netherlands: Elsevier, 2005.
- [45] S. Polychronopoulos and G. Memoli, "Acoustic levitation with optimized reflective metamaterials," *Sci. Rep.*, vol. 10, no. 1, pp. 1–10, Dec. 2020, doi: [10.1038/s41598-020-60978-4](https://doi.org/10.1038/s41598-020-60978-4).
- [46] Z. Yang, H. M. Dai, N. H. Chan, G. C. Ma, and P. Sheng, "Acoustic metamaterial panels for sound attenuation in the 50–1000 Hz regime," *Appl. Phys. Lett.*, vol. 96, no. 4, 2010, Art. no. 41906, doi: [10.1063/1.3299007](https://doi.org/10.1063/1.3299007).
- [47] S. Polychronopoulos, D. Kougiaris, P. Polykarpou, and D. Skarlatos, "The use of resonators in ancient Greek theatres," *Acta Acustica United With Acustica*, vol. 99, no. 1, pp. 64–69, Jan. 2013, doi: [10.3813/AAA.918589](https://doi.org/10.3813/AAA.918589).
- [48] S. L. Vassilantonopoulos and J. N. Mourjopoulos, "A study of ancient Greek and Roman theater acoustics," *Acta Acustica United With Acustica*, vol. 89, no. 1, pp. 123–136, 2003.

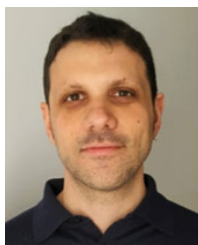


SPYROS POLYCHRONOPOULOS received the B.Sc. degree in physics from Patras University, Greece, and the Ph.D. degree from the Department of Mechanical and Aeronautical Engineering, Patras University.

From 2014 to 2017, he worked in London, U.K., as an Acoustic Consultant then moved to Brighton, U.K., where he worked for two years as a Research Fellow at the Department of Informatics, Sussex University, in a European Union funded project on acoustic levitation. He is currently a Research Fellow and a fixed-term Lecturer at the Department of Informatics and Telecommunications, National and Kapodistrian University of Athens. Since 1997, he has been composing music and he has released 15 albums. He has created his own algorithms to compose and unique electroacoustic interfaces to distribute his music. His research interests include ultrasound, and digital processing of audio and acoustic signals. He is a member of the Audio Engineering Society, the Institute of Acoustics, the Hellenic Institute of Acoustics, and the Hellenic Electroacoustic Music Composers Association.



DIMITRA MARINI was born in Athens, Greece, in 1994. She received the B.Sc. degree from the Department of Informatics and Telecommunications (DIT), National and Kapodistrian University of Athens (NKUA), Greece, in 2018. Since 2018, she has been a Research Assistant at DIT, NKUA. Her research interest includes the physical modeling of musical instruments.



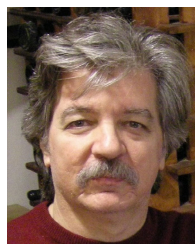
KONSTANTINOS BAKOGIANNIS received the M.E. degree in electrical and computer engineering from the National Technical University of Athens (NTUA), Greece, the M.A. degree in musicology from the National and Kapodistrian University of Athens (NKUA), Greece, and the Ph.D. degree in music informatics from the School of Electrical and Computer Engineering, NTUA.

He is a researcher in the field of sound and music computing. He is currently a Research Fellow at the Department of Informatics and Telecommunications, NKUA. He is also a classical-trained musician, holding degrees in piano performance, classical music theory, and composition issued by the Greek Ministry of Culture. His research interests include computational musicology, computer music, interactive dance, and physical modeling of musical instruments. Besides research, he is an active musician and composer.



GEORGIOS TH. KOUROUPETROGLOU (Member, IEEE) received the B.Sc. degree in physics and the Ph.D. degree in communications and signal processing from the National and Kapodistrian University of Athens (NKUA), Greece.

He has served as the Director of postgraduate studies and the Director of the Communication and Signal Processing Division at the Department of Informatics and Telecommunications, NKUA. He is currently a Professor and the Chairman of the Department of Informatics and Telecommunications, the Director of the Speech and Accessibility Laboratory, the Head of the Accessibility Unit for Students with Disabilities, and the Director of the M.Sc. programme in language technology at NKUA. His research interests include computer accessibility and voice user interfaces, as a part of the major domain of human-computer interaction. He is a member of the Editorial Board of the journals: *Universal Access in the Information Society* and *Technology and Disability*.



STELIOS PSAROUDAKĒS received the B.Sc. degree (Hons.) in mechanical engineering-naval architecture from University College London, the postgraduate Diploma degree in measurement and control of fluids from Surrey University, the Piano Recital Diploma degree from Ódeion Athēnōn, the MMus degree in ethnomusicology from Goldsmiths' College London, and the Ph.D. degree in classics-music from Reading University.

He is currently an Assistant Professor of ancient Hellenic music at the Department of Music Studies, National and Kapodistrian University of Athens. His research interests include ancient Hellenic music, especially organology (Chelys, Kithara, Aulos, and Plagiaulos), musical notation and surviving scores (parasēmantikē), theory of melody (harmonikē) and rhythm (rhythmikē), music in tragedy, and history of ancient Hellenic music. He is a member of the Moisa, the international society for the study of Greek and Roman music and its cultural heritage, Ravenna, and the ISGMA, the international study group on music archaeology, Berlin.



ANASTASIA GEORGAKI received the master's and Ph.D. degrees in music technology and musicology from IRCAM, in collaboration with EHESS, Paris, in 1991 and 1998, respectively. She has been the Head of the Department of Music Studies, since 2019; the Director of the Laboratory of Music Acoustics and Technology; and the Head of the postgraduate program "Music Technology and Contemporary Practices." She is currently a Professor of music technology at the Department

of Music Studies, School of Philosophy, National and Kapodistrian University of Athens. She has organized a large number of international and Greek music technology conferences. She has in her assets books, articles in Greek and foreign journals, international conference proceedings and collective volumes on the systematic dimension of the use of new technologies in music performance, creation and education, and musicological research. Her research interests include systematic musicology through acoustic analysis of the singing voice, synthesis of the singing voice, prosodic models of singing, biomusicological models, aesthetics and ethics of music technology in contemporary research, and systematic study of technological models in music creation. She is a member of the Sound and Music Computing Conference (SMC) steering committee and the Hellenic Musicological Society.

• • •